HHS Public Access

Author manuscript

Neuron. Author manuscript; available in PMC 2016 June 17.

Published in final edited form as:

Neuron. 2015 June 17; 86(6): 1393–1406. doi:10.1016/j.neuron.2015.05.033.

Reduction of Neuropathic and Inflammatory Pain through Inhibition of the Tetrahydrobiopterin Pathway

Alban Latremoliere[1], **Alexandra Latini**[1,2], **Nick Andrews**[1], **Shane J. Cronin**[1,3], **Masahide Fujita**[1], **Katarzyna Gorska**[4], **Ruud Hovius**[4], **Carla Romero**[1], **Surawee Chuaiphichai**[5], **Michio Painter**[1], **Giulia Miracca**[1], **Olusegun Babaniyi**[1], **Aline Pertile Remor**[1,2], **Kelly Duong**[1], **Priscilla Riva**[6], **Lee B. Barrett**[1], **Nerea Ferreirós**[7], **Alasdair Naylor**[8], **Josef M. Penninger**[3], **Irmgard Tegeder**[7], **Jian Zhong**[9], **Julian Blagg**[10], **Keith M. Channon**[5], **Kai Johnsson**[4], **Michael Costigan**[6,11,*], and **Clifford J. Woolf**[1,11,*]

[1]Kirby Neurobiology Center, Boston Children's Hospital and Department of Neurobiology, Harvard Medical School, Boston, MA 02115, USA [2]LABOX, Universidade Federal de Santa Catarina, 88040-900 Florianópolis, Brazil [3]Institute of Molecular Biotechnology of the Austrian Academy of Sciences, 1030 Vienna, Austria [4]Institute of Chemical Sciences and Engineering, École Polytechnique Fédérale de Lausanne, 1015 Lausanne, Switzerland [5]Department of Cardiovascular Medicine, University of Oxford, John Radcliffe Hospital, Oxford OX3 9DU, UK [6]Department of Anesthesia, Boston Children's Hospital and Department of Neurobiology, Harvard Medical School, Boston, MA 02115, USA [7]Pharmazentrum Frankfurt, Institut für Klinische Pharmakologie, Klinikum der Goethe-Universität, Theodor Stern Kai 7, 60590 Frankfurt am Main, Germany [8]The Canterbury Consulting Group, Unit 43 Canterbury Innovation Centre, University Road, Canterbury, Kent CT2 7FG, UK [9]Burke Medical Research Institute and Brain and Mind Research Institute, Weill Medical College of Cornell University, White Plains, NY 10605, USA [10]The Institute of Cancer Research, London SW7 3RP, UK

SUMMARY

Human genetic studies have revealed an association between GTP cyclohydrolase 1 polymorphisms, which decrease tetrahydrobiopterin (BH4) levels, and reduced pain in patients. We now show that excessive BH4 is produced in mice by both axotomized sensory neurons and macrophages infiltrating damaged nerves and inflamed tissue. Constitutive BH4 overproduction in sensory neurons increases pain sensitivity, whereas blocking BH4 production only in these cells reduces nerve injury-induced hypersensitivity without affecting nociceptive pain. To minimize risk of side effects, we targeted sepiapterin reductase (SPR), whose blockade allows minimal BH4 production through the BH4 salvage pathways. Using a structure-based design, we developed a potent SPR inhibitor and show that it reduces pain hypersensitivity effectively with a concomitant decrease in BH4 levels in target tissues, acting both on sensory neurons and macrophages, with no

*Correspondence: michael.costigan@childrens.harvard.edu (M.C.), clifford.woolf@childrens.harvard.edu (C.J.W.).
[11]Co-senior author

SUPPLEMENTAL INFORMATION

Supplemental Information includes Supplemental Experimental Procedures and seven figures and can be found with this article online at http://dx.doi.org/10.1016/j.neuron.2015.05.033.

development of tolerance or adverse effects. Finally, we demonstrate that sepiapterin accumulation is a sensitive biomarker for SPR inhibition in vivo.

INTRODUCTION

Most putative analgesic compounds tested over the last decade have failed in phase II trials due to lack of efficacy, even though they have robust preclinical activity (Arrowsmith and Miller, 2013; Woolf, 2010). One strategy to improve chances of translational success is to select a target or pathway for drug development with strong human genetic support. For example, patients carrying rare Mendelian recessive loss-of-function mutations for the sodium channel $Na_V1.7$ are completely indifferent to pain (Dib-Hajj et al., 2013), making this channel a potential target for eliminating acute pain sensitivity (Lee et al., 2014). Although informative for nociceptive pain, rare Mendelian conditions with large phenotypes may not be effective for selecting druggable targets for chronic pathological conditions, such as neuropathic pain and chronic inflammatory disease, as the chance of associating a diminished disease phenotype with a rare polymorphism is extremely low if the phenotype only manifests in the disease state, such as after a nerve lesion (Bennett and Woods, 2014; Costigan et al., 2012). An alternative approach is to identify relatively common genetic polymorphisms with smaller effect sizes on pain outcome in disease conditions, ideally with no effect on nociceptive pain, as these may reveal potential ways to alter specific molecular mechanisms responsible for pathological pain while leaving the protective aspects of acute pain intact.

SNP association studies carried out in 12 independent cohorts of patients have associated several polymorphisms within or close to the gene for GTP cyclohydroxylase 1 enzyme (GTPCH1; hereafter named GCH1) with reduced clinical and experimental pain sensitivity (Belfer et al., 2014; Kim et al., 2013; Latremoliere and Costigan, 2011). GCH1 catalyzes the initial and rate-limiting step in the synthetic pathway of the pteridin (6R)-L-erythro-5,6,7,8-tetrahydrobiopterin (BH4). BH4 is an essential cofactor for aromatic amino acid hydroxylases, nitric oxide synthases (NOSs), and alkylglycerol monooxygenase, making it indispensable for synthesis of serotonin, epinephrine, norepinephrine, dopamine, nitric oxide, and metabolism of glycerolethers (Werner et al., 2011). That particular polymorphisms in GCH1 are associated with less clinical pain without CNS adverse effects or disruption of nociception represents a functional outcome that would be highly desirable to replicate pharmacologically.

A general challenge of human genetic association studies is how to reverse engineer the discovery of a polymorphic gene associated with a desirable clinical outcome into a druggable target supported by robust mechanistic validation in model organisms. Expression and functional profiling in rodents has shown that enhanced GCH1 transcription and activity in injured sensory neurons lead to increased BH4 levels, which results in greater pain hypersensitivity, and conversely that inhibiting this enzyme’s function reduces pain (Kim et al., 2009; Nasser et al., 2013; Tegeder et al., 2006). Crucial questions remain, however; where and how do excess BH4 levels contribute to neuropathic and inflammatory pain and, from a translational perspective, can disruption of the synthesis of this critical cofactor

constitute a viable analgesic drug development strategy without generating unacceptable side effects?

To address these issues, we set out to determine where anatomically the BH4 pathway regulates the pain phenotype in vivo and the functional consequences of increased or decreased BH4 levels in sensory neurons. Finally, we pharmacologically targeted the terminal BH4 synthetic enzyme sepiapterin reductase (SPR) as a way of reducing pathologically elevated BH4. These murine studies define and validate a molecular pathway (BH4 synthesis) that contributes to pain hypersensitivity following nerve injury and inflammation and its locus of activation (injured neurons and macrophages), and from this reveal a specific target (SPR) for reducing elevated BH4 synthesis while minimizing adverse effect liability.

RESULTS

Cellular Localization of GCH1 in Injured Sensory Neurons

To identify cells that produce BH4 after peripheral nerve injury, we used bacterial artificial chromosome transgenic reporter mice in which GFP is expressed under control of the endogenous *Gch1* promoter, as *Gch1* expression is tightly correlated with BH4 production (Tatham et al., 2009). In naive reporter mice, the GFP signal was below detection levels in sciatic nerves and dorsal root ganglia (DRGs), indicating low basal *Gch1* transcriptional activity (Figures 1A and 1E). Seven days after injury to the sciatic nerve, numerous GFP-positive cells were detected in the proximal segment of the damaged nerve (Figure 1B). Increase in GCH1 levels was confirmed by western blot and enzyme activity (Figure 1C). Costaining with CD68 revealed that a large proportion of the GFP-positive cells were macrophages (Figure 1D). In lumbar level (L)3 and L4 DRGs ipsilateral to a sciatic injury a week before, neuronal *Gch1* transcriptional activity also increased, as detected by increased GFP signal and enzyme activity (Figure 1F). A soma size distribution analysis showed a mixed population of small- (<30 μm), medium- (30–40 μm), and large- (>40 μm) diameter GFP^+ DRG neurons after injury (Figure 1G). Costaining with specific molecular markers revealed that only axotomized neurons ($ATF3^+$) showed elevated expression of *Gch1* after the nerve injury (Figure 1H), and that these included myelinated ($NF200^+$) and unmyelinated ($NF200^-$) neurons. Among the unmyelinated neuronal population, both peptidergic ($CGRP^+$, SP^+, and $TRPV1^+$) and nonpeptidergic ($IB4^+$) neurons expressed *Gch1* (Figures 1I–1L). Together, these results indicate that after a peripheral nerve injury, *Gch1* transcription is upregulated both in macrophages in the nerve proximal to the injury and in injured neurons, including all major sensory neuron classes. The proportion of neurons expressing *Gch1* 21 days after spared nerve injury (SNI) was similar to that found at 7 days (Figure S1A), indicating that elevated transcription persists for some time after injury.

Regulation of BH4 Synthesis, Recycling, and Salvage Pathways after Peripheral Nerve Injury

Cellular levels of BH4 are determined by the combined action of de novo synthesis, recycling, and salvage pathways (Figure 1M). We therefore measured changes following sciatic nerve injury in the expression of transcripts for enzymes in all these three pathways

in the nerve and DRG. In addition to *Gch1*, which was upregulated in injured nerves and DRGs at each time point tested, we also found upregulation of carbonyl reductase 2 (*Cbr2*) in the two tissues. Dihydrofolate reductase (*Dhfr*), a salvage pathway enzyme, was transiently upregulated in the DRG, but exhibited a more sustained increase in the injured nerve. None of the enzymes related to BH4 production changed their transcript profiles in the dorsal horn of the spinal cord (Figure 1N). Collectively, the increase in the expression of the transcripts for these enzymes correlates with an elevation in biopterin levels (an oxidized biomarker of BH4) in the DRGs and in proximal injured nerves (Figure 1O). These results indicate that several enzymes involved in BH4 production are upregulated in the mouse after peripheral nerve injury, and that BH4 levels are increased not only in the DRGs, as previously reported in the rat (Tegeder et al., 2006), but also in infiltrating immune cells of the injured sciatic nerve.

Forced Expression of GCH1 in Sensory Neurons Increases Pain Sensitivity in Naive Mice

To test whether increasing BH4 levels specifically in sensory neurons can enhance pain sensitivity in naive animals, we generated a *Cre*-recombinase-dependent *GCH1* overexpressor mouse line. These animals contain a transgene that expresses the human *GCH1* gene tagged with an influenza hemagglutinin (HA) tag under the human cytomegalovirus early enhancer/chicken β-actin (CAG) promoter in cells (Figure 2A). We crossed these animals with a sensory neuron-specific *Advillin-Cre* line (Hasegawa et al., 2007) to generate *GCH1*-HA-overexpressing (OE) mice in all sensory neurons, as revealed by immunostaining of the HA tag and the size distribution of HA-positive cells (Figures 2A and 2B). Overexpression of the transgene was also observed by western blot using antibodies directed against GCH1 or the HA tag in the sciatic nerve and DRG (Figure 2C). Measurement of enzyme activity and biopterin levels in the DRGs of these mice showed that overexpression of *GCH1* led to increased GCH1 activity and BH4 overproduction (Figures 2D and 2E).

The genetically engineered constitutive overexpression of BH4 selectively in sensory neurons caused increased nocifensive responses upon intraplantar injection of the TRPV1 agonist capsaicin (Figure 2F) and a heightened sensitivity to radiant (Figure 2G) and contact heat (Figure S2A), whereas mechanical sensitivity, tested by von Frey filaments and calibrated forceps, did not differ from littermates (Figures S2B and S2C). These results suggest that BH4 overexpression in naive animals mainly affects the sensitivity of C fiber nociceptor neurons responsive to heat and chemical stimuli. To confirm this, we crossed the conditional *GCH1*-HA OE line with *Na(v)1.8*$_{Tg}$-*Cre* transgenic animals, where *Cre* expression is restricted to small-diameter neurons (Agarwal et al., 2004). As expected, GCH1-HA was expressed only in small sensory neurons (Figures 2H and 2I). Protein levels of GCH1-HA, enzyme activity, and biopterin levels were significantly increased in the *Na(v)1.8*$_{Tg}$-*GCH1*-HA OE animals compared to their littermates, both in the sciatic nerve and DRG (Figures 2J–2L). The nociceptive pain profile of these mice fully phenocopied that of the *Advillin-GCH1*-HA OE animals, indicating that restricting overexpression of BH4 to small-caliber fibers is sufficient to cause a hypersensitivity to noxious heat and capsaicin (Figures 2M and 2N; Figures S2D–S2F). Because BH4 sensitizes TRPV1 channels through nitrosylation in vitro (Miyamoto et al., 2009), we administered L-NG-nitroarginine methyl

ester (L-NAME; 50 mg/kg intraperitoneally [i.p.], a dose that fully blocks NOS activity; Moore et al., 1993) to the *Advillin-GCH1*-HA OE mice. This treatment normalized the radiant heat responses to levels similar to littermates (Figure 2O). These results imply that BH4 is acting in a cell-autonomous fashion—changing neural function where its levels are increased. To test whether BH4 overexpression affected the detection of nonnoxious temperatures, we used thermal gradient paradigms (Moqrich et al., 2005). *Na(v)1.8*$_{Tg}$-*GCH1*-HA overexpressor mice and their littermates both settled at 32°C within an hour, indicating no effect of BH4 overexpression on innocuous thermodetection (Figure 2P; Figure S2G). Finally, we also tested whether a short-term exposure to increased GCH1 activity in neurons was sufficient to heighten heat pain sensitivity. To evaluate this, we used an inducible sensory-neuron-specific *Brn3a-Cre*ER^{T2} mouse (O'Donovan et al., 2014). Tamoxifen administration (1 mg per mouse i.p. for 5 days) induced *GCH1*-HA in all sensory neurons observed 1 week after the end of treatment (Figure 2Q), and the mice developed hypersensitivity to contact heat (Figure 2R) but not to von Frey filaments (Figure S2H).

We conclude that an increase in BH4 synthesis in uninjured DRG neurons is sufficient to produce heightened heat pain sensitivity, and that this occurs in this context through increased NO synthesis.

Loss of GCH1 in Sensory Neurons Attenuates Neuropathic Pain

Next, we tested whether specifically preventing BH4 upregulation in sensory neurons after a nerve injury diminished the neuropathic pain phenotype. Because *Gch1* is upregulated in myelinated and unmyelinated neurons after peripheral nerve injury, we crossed the *Advillin-Cre* driver line with mice in which exons 2 and 3 of the *Gch1* gene are flanked by flox sequences (Chuaiphichai et al., 2014). These exons code the active site of the enzyme, and their excision by *Cre* led to a large decrease of enzymatic activity in DRG tissue and cultures of primary sensory neurons (Figure 3A). GCH1 activity was also reduced in the intact sciatic nerve (Figure 3B), implying that GCH1 present in naive animals has a predominant sensory neuronal origin and is likely axonally transported, as reported in the brain (Levine et al., 1981). No differences were observed in the responses to radiant or contact heat, capsaicin, von Frey filaments, or calibrated forceps (Figures 3C–3G) in naive *Advillin-Gch1* knockout (KO) animals when compared to their littermates, indicating that active BH4 synthesis in sensory neurons is not necessary for nociceptive pain.

After peripheral nerve injury (SNI model), *Advillin-Gch1* KO mice did not display the increase in biopterin levels in DRGs observed in littermates after such lesions (Figure 3H) and exhibited significantly reduced mechanical sensitivity (higher thresholds) throughout the 3 weeks of testing (Figure 3I), but showed no difference in the response to cold produced by acetone evaporation (Figure S3A). A similar reduced mechanical hypersensitivity was also observed when *Advillin-Gch1* KO mice were subjected to the chronic constriction injury (CCI) model of peripheral neuropathic pain (Figure S3B). Elevated *Gch1* mRNA was still evident in the injured sciatic nerve of the *Advillin-Gch1* KO SNI mice, showing that in the damaged nerve, Gch1 synthesis is largely nonneuronal in origin (Figure 3J), likely mainly macrophages (Figures 1B and 1D), and this was supported by increased BH4 in the injured

nerve of both WT and *Advillin-Gch1* KO mice (Figure 3K), which has, therefore, two sources: injured sensory neurons and infiltrating leukocytes, with the latter predominant.

To test whether blocking BH4 synthesis in sensory neurons could alleviate established neuropathic pain-like behaviors, we used inducible *Brn3a-Cre*ER^{T2} *Gch1* floxed mice. Immediately following nerve injury all mice developed identical levels of mechanical hypersensitivity, but tamoxifen treatment (1 mg per mouse i.p. for 5 days starting on day 7) resulted in an increase in threshold only in the *Brn3a-Cre*ER^{T2} *Gch1* KO mice from day 14 until testing ended on day 25 (Figure 3L).

Specific reduction of BH4 production in sensory neurons can then both prevent and alleviate, to a substantial but incomplete extent, established nerve injury-induced pain hypersensitivity. Because we found infiltrating immune cells to be a major source of BH4 in the damaged nerve after peripheral nerve injury, we next sought to reduce BH4 production in both cell types by genetic and pharmacological means, to test whether this could further reduce neuropathic pain hypersensitivity.

Pharmacological Inhibition of BH4 Synthesis and Reduced Pain Hypersensitivity

The only known inhibitor of GCH1 is 2,4-diamino-6-hydroxypyrimidine (half-maximal inhibitory concentration [IC_{50}] ~300 μM; Kolinsky and Gross, 2004), which produces analgesia in rats (Pickert et al., 2012; Tegeder et al., 2006). GCH1 is the obligate and rate-limiting step for BH4 production and, as a consequence, its complete inhibition for extended periods would prevent any new BH4 synthesis, likely precipitating side effects due to reduced levels of biogenic amines and NO synthesis. Furthermore, the GCH1 complex is not a readily tractable drug target because of the lack of accessible active sites, which point inward in a dipentameric barrel-like structure (Nar et al., 1995a, 1995b).

We therefore considered another enzyme within the BH4 synthesis cascade, sepiapterin reductase, the terminal enzyme in the de novo synthesis pathway, as a potential target for reducing pathologically elevated BH4 levels. X-ray crystallography has revealed a clear pocket for its known inhibitor *N*-acetylserotonin (NAS; Auerbach et al., 1997; Naylor et al., 2010; Smith et al., 1992), opening opportunities to look for other inhibitors. NAS has an IC_{50} of ~50 mM (Chidley et al., 2011) but is also an intermediate in melatonin production, making systemic use unfeasible (Tegeder et al., 2006). Recently, sulfasalazine (SSZ), an Food and Drug Administration-approved anti-inflammatory compound, was found in a yeast three-hybrid screen to inhibit SPR activity through its metabolite sulfapyridine (IC_{50} ~200 μM; Haruki et al., 2013). Given the production of excess BH4 in sensory neurons and in infiltrating macrophages, we decided to test whether this anti-inflammatory agent reduced pain-related hypersensitivity in mice after SNI. Because intestinal flora metabolizes sulfasalazine into sulfapyridine (which otherwise has a poor solubility), we administered sulfasalazine (50 mg/kg) by gavage twice a day for 3 days, beginning 7 days after SNI. With this regime, SSZ on the third day of administration modestly reduced mechanical hypersensitivity for 2 hr with a maximum effect at 1 hr (Figure S3C).

The limited bioavailability, low potency, and complex metabolism of SSZ did not allow direct analysis of the relationship between BH4 levels and reduced pain-like behavior. We

therefore used structure-based design to produce a more potent SPR inhibitor, guided by the crystal structure of mouse SPR in complex with NAS (PDB: 1NAS; Auerbach et al., 1997) and previous work on this scaffold by Smith et al. (1992) and designed the compound illustrated in Figure 4A, *N*-(2-(5-hydroxy-2-methyl-1H-indol-3-yl)ethyl)-2-methoxyacetamide, which we named SPRi3 as the third SPR inhibitor (after NAS and SSZ). Compared to NAS, SPRi3 has an additional methyl group at the 2-position of the indole scaffold to allow for additional hydrophobic interactions and a methoxyacetyl group instead of the acetyl group, as it has been shown that the latter modification significantly increases the affinity of NAS toward SPR (Smith et al., 1992). SPRi3 displayed very high binding affinity to human (h)SPR in a cell-free assay (IC_{50} 74 nM versus 1.9 μM for NAS; Figure 4B) and efficiently reduced biopterin levels in a cell-based assay (IC_{50} 5.2 μM versus 54 mM for NAS; Figure 4C), consistent with good cell permeability (Caco-2: Papp A to B: 10.7 × 10^{-6} cm•s^{-1}; efflux ratio 1.4). SPRi3 also significantly reduced SPR activity in mouse primary cultures of sensory neurons (IC_{50} 0.45 μM; Figure 4D) without affecting the activity of GCH1 (Figure S4A).

We then solved the crystal structure of hSPR in complex with SPRi3 and NADPH (PDB: 4XWY). As observed for NAS, the 5-hydroxy group of SPRi3 is anchored via hydrogen bonding to the conserved Asp254 (Figure 4E; Figure S4). The side chain of SPRi3 penetrates deep into the substrate-binding site, where its *cis*-amide bond forms hydrogen bonds with catalytic residues Ser154 and Tyr167 (Figure 4E). This is in contrast to the structure of NAS bound to SPR, where no hydrogen bonds between the amide bond and the active-site residues are formed (Figure S4B). The methoxyacetyl group of SPRi3 makes extensive hydrophobic interactions with Met202 and Gln203, and the 2-methyl group of the indole scaffold makes hydrophobic contacts with residue Leu219. Evidently, SPRi3 fits very well in the substrate-binding site of hSPR (Figure 4F). In contrast to the structures of sulfa drugs bound to SPR, there is little direct interaction between SPRi3 and the cofactor NADPH (Figure S4C). Overall, the structure of the ternary complex of SPRi3, NADPH, and SPR explains both the exquisite binding affinity of SPRi3 and why it is a more potent SPR inhibitor than NAS. When administered to mice i.p. at 300 mg/kg, plasma levels of SPRi3 had a rapid (T_{max} 0.11 hr) and short exposure, an elimination half-life of 3.95 hr (Figure 4G) with low plasma protein binding (11.6%).

Whereas under normal conditions SPR mediates the conversion of its substrate 6-pyruvoyl-tetrahydropterin to BH4, in the absence of enzyme activity due, for example, to genetic mutation, low-level production of BH4 can still be achieved through the salvage pathway in various cell types (Figure 4H; Bonafé et al., 2001; Hirakawa et al., 2009; Thöny and Blau, 2006). This could act to prevent excessive global depletion of basal levels of BH4 during SPR inhibition. The sequential action of the enzymes aldose reductase (AKR1B1)/carbonyl reductase (CR) and dihydrofolate reductase (DHFR) involves the nonenzymatic production of sepiapterin from 2′-hydroxy-1′-oxopropyltetrahydropterin (1′oxoPH4; Figure 4H). Sepiapterin does not normally accumulate, because SPR reduces 1′oxoPH4 into BH4, and this metabolite is therefore not an endogenous substrate for this enzyme (Milstien and Kaufman, 1989; Nichol et al., 1983). Because sepiapterin is chemically stable its accumulation could, however, represent a biomarker of SPR inhibition, and indeed we found

that sepiapterin levels increased concomitantly with SPR inhibition in cultured DRG neurons (Figure 4I). Sepiapterin levels were undetectable both in normal states and when the de novo pathway activity was increased by interleukin (IL)-1β, whereas application of SPRi3 caused a concentration-dependent increase in the metabolite (Figure 4I). When SPRi3 was administered in vivo, sepiapterin levels in plasma correlated highly with those of SPRi3 ($r = 0.9166$), confirming its utility as a biomarker for sepiapterin reductase inhibition (Figure 4J). SSZ treatment also increased plasma levels of sepiapterin (Figure S4D). These data confirm in vivo target engagement of both SSZ and SPRi3 as SPR inhibitors.

SPRi3 administered at 100, 200, or 300 mg/kg (i.p.) produced a dose-dependent antitactile allodynic effect in mice in the SNI model of neuropathic pain, with a maximum response 1 hr after injection (Figure 5A). At this dose, SPRi3 also reduced mechanical allodynia in mice with a different neuropathic pain model, chronic constriction injury, with a similar time course (Figure 5A). One hour after injection of the most efficacious dose (300 mg/kg), SPRi3 was detected in both injured sciatic nerves and DRGs of SNI mice, and this was associated with a reduction in SPR activity and an increase in sepiapterin levels, as well as reduction in BH4 levels in these two tissues (Figures 5B and 5C). Administration of SPRi3 in naive mice did not affect nociceptive pain (Figures S5B–S5D).

To determine whether the antiallodynic effect of SPRi3 in the SNI pain model was solely mediated through inhibition of SPR in sensory neurons, we administered it to *Advillin-Gch1* KO mice after SNI. SPRi3 produced a modest but significant further antiallodynic effect for an hour after injection, on top of the already reduced pain-like sensitivity of these animals (Figure 5D). These results suggest that systemic SPR inhibition has an action other than just on sensory neurons, such as on macrophages in the injured nerve (Figure 1D). To evaluate this, we assessed the effect of SPR blockade on macrophages in vitro. SPRi3 (50 μM) added to purified peritoneal macrophages activated by lipopolysaccharide (LPS) (5 μg/ml) for 24 hr or LPS followed by 1 hr ATP (1 mM) prevented NO generation but not proinflammatory cytokine (IL-1β and IL-6) production (Figure 5E; Figure S5E), indicating action of the inhibitor on specific aspects of this immune cell's function.

To test whether SPR inhibition alleviates mechanical allodynia in a fully established neuropathic pain state, we administered SPRi3 to mice at 2, 3, or 4 weeks after the start of the SNI model and after 6 weeks in the CCI model. Relative treatment efficacy remained the same at each time point tested in both models (Figure 6A; Figure S6A), indicating that BH4 production continues to contribute to neuropathic pain at these later time points. Single administration of SPRi3 produced no effect on motor coordination (Figure 6B), voluntary motor activity (Figure S6B), the holeboard test (a paradigm sensitive to dopaminergic defects; Figure 6C; Figure S6C), or the tail suspension test (sensitive to serotonin defects; Figure S6D). Acute administration of SPRi3 reduced plasma BH4 levels without affecting systolic blood pressure and heart rate (Figure 6D; Figures S6E–S6H). When injected repeatedly (two injections per day for 3 days), SPRi3 produced similar antiallodynic effects after the first and last injections (Figure 6E), indicating no tolerance. Under this dosage regime the mice displayed no obvious adverse effects (no change in appearance, weight, or general activity), and exploration behaviors assessed by the holeboard test were not altered (Figure 6F). In addition, serotonin and dopamine levels remained unchanged in the striatum

and hippocampus (Figure 6G; Figure S6I). Although SPR activity was reduced in the liver (Figure 6H), as reflected by an increase in sepiapterin levels (Figure 6I), phenylalanine plasma levels were not changed throughout the treatment period (Figure 6J), showing that sufficient levels of BH4 were maintained, despite the SPR inhibition, to metabolize phenylalanine. The difference in sepiapterin levels in plasma produced by an effective analgesic dose of SPRi3 (300 mg/kg) and an ineffective one (100 mg/kg) was sufficient that this could be used as a biomarker of efficacy (Figure 6K).

The expression of *Gch1* in and effects of SPRi3 on macrophage function, as well as the activity of SSZ in rheumatoid arthritis (O'Dell et al., 2013), led us to assess whether SPRi3 could reduce inflammatory pain hypersensitivity, where these cells play an important role (Marchand et al., 2005). Using *Gch1*-eGFP mice, we found that intraplantar injection of complete Freund's adjuvant (CFA; 20 μg) caused infiltration of macrophages within the paw, many of which expressed *Gch1* (Figure 7A). SPRi3 (300 mg/kg i.p.) significantly attenuated for 1 hr the thermal hyperalgesia produced by intraplantar CFA 1 day before (Figure 7B; Figure S7A) without affecting mechanical allodynia (Figure S7B), and this was associated with a decrease in BH4 levels in the inflamed paw (Figure 7C). The development of thermal hyperalgesia after intraplantar injection of CFA was not significantly affected in sensory neuron-specific *Gch1* KO mice (Figure 7D), suggesting that BH4 produced by immune cells contributed to pain hypersensitivity in this model.

We next administered CFA (20 μg) to the knee joint as a model of rheumatoid arthritis. SPRi3 injection (300 mg/kg i.p.) significantly improved weight-bearing defects for at least 1 hr when administered 2, 3, and 4 days after CFA injection, but not on day 1 (Figure 7E). Interestingly, under this daily SPRi3 injection regime, knee thickness (a measure of inflammatory swelling) resolved faster than in vehicle-injected animals (Figure 7F), suggesting an anti-inflammatory action of the treatment. In support of this, a preemptive paradigm where SPRi3 was first administered 1 hr before CFA partially prevented the full establishment of knee thickness and pain hypersensitivity the next day (Figure 7G; Figure S7C).

Systemic administration of an SPR inhibitor reduces BH4 production following peripheral nerve damage and inflammation, and this alleviates pain-like hypersensitivity in mice through effects on sensory neurons and macrophages without tolerance, noticeable side effects, or disturbances in BH4-dependent metabolites, at least after short-term exposure.

DISCUSSION

We designed an approach to "reverse engineer" human genetic studies that have revealed an association between decreases in BH4 synthesis and reduced neuropathic (Costigan et al., 2012; Latremoliere and Costigan, 2011) and sickle cell disease pain (Belfer et al., 2014) into mechanistic analyses in mouse models. Animal models are critical to understand how, when, and where a pathway may drive a disease process and to assess therapeutic opportunities from inhibiting this pathway as well as liabilities that may occur from such inhibition. We used tissue-specific transgenic mice to formally demonstrate that BH4 modulates pain sensitivity in somatosensory neurons. We found that BH4 overproduction leads to an NO-

mediated heightened heat pain sensitivity in uninjured mice, whereas preventing BH4 production only in sensory neurons significantly attenuates the development of nerve injury-induced mechanical hypersensitivity. The ability to reduce symptoms once they are fully established is an essential prerequisite for any potential therapeutic applications of a novel target pathway. We therefore generated inducible sensory neuron-specific *Gch1* KO mice to show that blocking BH4 production is sufficient to partially reverse established hypersensitivity, indicating that BH4 is involved in maintaining the pain phenotype and, as a consequence, that targeting this pathway in injured peripheral neurons may have therapeutic utility.

In humans, the link between BH4 and pain was discovered through identification of a haplotype allele of *GCH1* that is both associated with reduced pain and decreased transcription of the *GCH1* gene and BH4 production following cellular stress (Tegeder et al., 2006) but without any of the major CNS, cardiovascular system (CVS), or metabolic effects found in patients with loss-of-function mutations in BH4 synthetic enzymes. These cause decreases in global BH4 levels below that required to maintain adequate NO and aromatic amine synthesis, as well as associated developmental defects (Bonafé et al., 2001; Douglas et al., 2015; Takazawa et al., 2008). The challenge then is how to reduce elevated BH4 in target tissues, such as sensory neurons and immune cells, without affecting excessively basal levels in the brain, endothelial cells, and liver. Because GCH1 is an obligate enzyme in the de novo synthetic pathway, its inhibition would cumulatively reduce BH4 levels as metabolites in the salvage and recycling pathways were used up. We therefore targeted another enzyme in the de novo BH4 synthesis pathway, SPR, downstream of GCH1. Although this enzyme shows little transcriptional change after nerve injury and so far has no described polymorphisms associated with altered pain sensitivity, we hypothesized that it may represent a more reasonable target to modulate BH4 production to produce pain relief than GCH1. We hypothesized that systemic SPR blockade would reduce nerve injury-induced BH4 overproduction without fully blocking BH4 production in normal tissue, because SPR's substrate 6-pyruvoyl-tetrahydropterin can be converted into BH4 through the salvage pathway, including metabolism of sepiapterin, whose level we predicted would increase with SPR inhibition. In human SPR loss-of-function mutations, several cell types in peripheral tissues show such a diversion of BH4 synthesis, and although these alternate synthesis routes are less effective than the de novo synthesis pathway, they allow sufficient BH4 production for maintaining baseline activity of enzymes requiring this cofactor (Bonafé et al., 2001; Hirakawa et al., 2009). Supporting such rescue of BH4 synthesis via these pathways, we found that, although systemic administration of an SPR inhibitor reduced BH4 levels in the DRG and injured nerve sufficiently to reduce nerve injury-induced hypersensitivity, it produced none of the side effects expected from global BH4 deficiency (Thöny and Blau, 2006). Cardiovascular and behavioral parameters particularly sensitive to NO, 5-hydroxytryptamine (5-HT), or dopamine deficit were not altered and brain amine levels remained unchanged after acute or repeated administration of the SPR inhibitor. Furthermore, SPR inhibition in the liver was not associated with increased phenylalanine levels, indicating that sufficient BH4 levels were present in this tissue to allow phenylalanine hydroxylase function. These results are in line with the safety profile of sulfasalazine in patients, which produces very few CNS, CVS, or metabolic side effects,

even when administered chronically at high doses (Costigan et al., 2012). The pharmacological blockade of SPR maintained the same relative efficacy for alleviating nerve injury-induced hypersensitivity when tested at multiple times after injury, suggesting that repeated treatment with an SPR inhibitor is possible without pharmacological tolerance.

The degree of pain relief produced after systemic inhibition of SPR was greater than that achieved after a *Gch1* knockout restricted to sensory neurons, which we interpret as indicating that additional cell types produce BH4 after peripheral nerve injury to generate pain and these are inhibited by SPR inhibitor treatment. We found an infiltration of *Gch1*-expressing macrophages into the damaged nerve, and this represents a novel and unsuspected source for BH4 production after peripheral nerve injury and for participation in the generation of neuropathic pain. Macrophages infiltrating the damaged nerve could produce several BH4-dependent molecules that might potentially sensitize nociceptor fibers and contribute to neuropathic pain hypersensitivity. One such factor is NO (Gorren and Mayer, 2002), and indeed we find that SPR inhibition in vitro blocked NO production in macrophages. We found evidence for a contribution of NO to the heat pain hypersensitivity resulting from high constitutive BH4 levels in sensory neurons, but BH4 can also produce a non-NO-mediated sensitization of nociceptors (Nasser et al., 2015), indicating that this cofactor may modify pain via diverse mechanisms in different pathological circumstances. For example, serotonin, whose synthesis is dependent on BH4 (Friedman et al., 1972), sensitizes nociceptors through the activation of 5-HT_{2A} (Okamoto et al., 2002) and 5-HT_3 receptors (Kayser et al., 2007). Lowering production of 5-HT in peripheral tissues by reducing BH4 could also participate in reducing pain hypersensitivity.

Because NOS1 (macrophages) and NOS2 (neurons) have a cumulative effect on pain hypersensitivity (Guan et al., 2007; Kuboyama et al., 2011), it is possible that systemic inhibition of SPR alleviates mechanical allodynia by decreasing activity in both these enzymes in the two cell types, and the dual action of the SPR inhibitor on neurons and immune cells may explain its broad efficacy profile for neuropathic and inflammatory pain. BH4 is involved in other aspects of macrophage function during inflammation, such as redox and antioxidant reactions (McNeill et al., 2015) and in regulation of their lipidome (Watschinger et al., 2015), so that reducing BH4 may produce multiple antiinflammatory effects. Supporting a proinflammatory involvement of BH4, we found that SPR inhibition in vivo reduced inflammatory swelling and pain hypersensitivity in two inflammatory pain models, each with strong involvement of macrophages (Marchand et al., 2005). These results are in agreement with clinical data reporting significant reductions in both pain and inflammation in rheumatoid arthritis and inflammatory bowel disease patients treated with sulfasalazine (Costigan et al., 2012). Macrophages play an important role in both rheumatoid arthritis (Kinne et al., 2007; Li et al., 2012) and inflammatory bowel disease (Heinsbroek and Gordon, 2009), and it is possible, therefore, that BH4 production in these cells contributes to the disease.

Current medications for neuropathic pain show relative efficacy in less than 50% of patients and cause disturbing side effects in many (Finnerup et al., 2005, 2010). One reason for this is the lack of quantifiable ways to titer doses for treatment efficacy versus side effects. Our results show that sepiapterin levels represent a reliable surrogate endpoint to quantify SPR

inhibition both in vitro and in vivo. We found a clear separation between plasma sepiapterin levels in mice treated with a suboptimal dose of SPR inhibitor and those treated with an effective antiallodynic dose without detectable adverse effects. It is conceivable that higher sepiapterin levels, indicating a greater degree of SPR inhibition, could also define a side-effect window, such as after high-dose prescriptions of sulfa-compound SPR inhibitors (Haruki et al., 2013). Because this metabolite is chemically stable, easily measured in plasma, and accumulates only when SPR is inhibited, this confers a high signal-to-noise ratio and specificity—critical properties for a biomarker (Wagner et al., 2007).

In conclusion, our data illustrate how one can utilize human genetics to discover a pathway involved in a disease and then through preclinical mechanistic studies identify and target the most suitable member of that pathway for drug development, even if it was not the primary point of cascade detection. Reducing BH4 production via SPR inhibition could represent a viable approach for normalizing neuropathic and inflammatory pain hypersensitivity, one that uniquely acts both on injured sensory neurons and activated macrophages, and where adverse effects may be limited by a salvage pathway that prevents excessive reduction of the essential cofactor by diversion of SPR's substrate to low-level BH4 synthesis by alternative pathways.

EXPERIMENTAL PROCEDURES

Genetic Gain- and Loss-of-Function Strategies

Mice expressing eGFP under the *Gch1* promoter were used to label cells that upregulate *Gch1* after SNI or CFA injection. Mice with a *Cre*-dependent *GCH1*-HA overexpression cassette produced BH4 overproduction, and *Gch1* floxed mice prevented BH4 production. For both gain- and loss-of-function experiments, we bred *GCH1*-HA and *Gch1* floxed mice with sensory neuron-specific *Advillin-Cre*, *Na(v)1.8*$_{Tg}$-*Cre*,, or the inducible *Brn3a-Cre*ER^{T2} animals. All animal procedures were approved by the Boston Children's Hospital Animal Care and Use Committee.

Behavioral Assessments and Chronic Pain Models

Behavioral experiments were done blind to genotype or treatment. High-threshold mechanical sensitivity was assessed by calibrated forceps, heat sensitivity by radiant and contact heat latencies, chemical nocifensive responses by intraplantar injection of capsaicin, and thermal detection by thermal gradient. For peripheral nerve injury, mice underwent SNI (Decosterd and Woolf, 2000) or CCI (Bennett and Xie, 1988). For inflammatory pain, mice received intraplantar or intraknee injection of CFA. In chronic models, mechanical allodynia thresholds were determined using von Frey filaments, cold allodynia by acetone evaporation, and movement-associated pain signs by dynamic weight bearing.

Biopterin/Sepiapterin/SPRi3 Concentrations

BH4, BH2, and biopterin samples were injected onto an isocratic HPLC system and quantified using sequential electrochemical (Coulochem III; ESA) and fluorescence detection (excitation 350 nm, emission 450 nm) (JASCO). Sepiapterin concentrations were

determined by liquid chromatography coupled to electrospray ionization tandem mass spectrometry.

Statistical Analysis

Results are expressed as mean ± SEM unless specified otherwise. Details of statistical assessment are in Supplemental Experimental Procedures.

Supplementary Material

Refer to Web version on PubMed Central for supplementary material.

ACKNOWLEDGMENTS

This work was supported by NIH R01NS58870 and R37NS039518 (C.J.W.), R01NS074430 (M.C.), the Foundation for Peripheral Neuropathy (C.J.W.), Boston Children's Technology Development Fund (C.J.W.), Anesthesia Trailblazer Award 2014 (M.C.), Mass Life Science Consortium (C.J.W. and M.C.), and the Neurodevelopmental Behavior Core and Pharmacokinetics Core, Boston Children's Hospital (P30 HD18655). A. Latremoliere was the recipient of a Fondation pour la Recherche Medicale fellowship and was partially supported by grant R01DE022912. A. Latini was a recipient of a Coordenação de Aperfeiçoamento de Pessoal de Nível Superior postdoctoral fellowship and is a research fellow of Conselho Nacional de Desenvolvimento Científico e Tecnológico (CNPq). A.P.R. was the recipient of a CNPq Sandwich doctoral scholarship. I.T. was supported by the Deutsche Forschungsgemeinschaft (SFB815, project A12). J.Z. was supported by Whitehall Foundation research grant 2010-08-61, 1R01EY022409, from the National Eye Institute. We wish to thank Sandra Labocha and Ashley Hale for technical assistance, Florence Pojer for instruction on crystallization and structure resolution, the beamline staff of the Swiss Light Source for support during X-ray data collection, and Merck Research Laboratories Boston and Gerard Berry and Xiaoping Huang from BCH for HPLC-MS/MS methodological support.

REFERENCES

Agarwal N, Offermanns S, Kuner R. Conditional gene deletion in primary nociceptive neurons of trigeminal ganglia and dorsal root ganglia. Genesis. 2004; 38:122–129. [PubMed: 15048809]

Arrowsmith J, Miller P. Trial watch: phase II and phase III attrition rates 2011–2012. Nat. Rev. Drug Discov. 2013; 12:569. [PubMed: 23903212]

Auerbach G, Herrmann A, Guütlich M, Fischer M, Jacob U, Bacher A, Huber R. The 1.25 Å crystal structure of sepiapterin reductase reveals its binding mode to pterins and brain neurotransmitters. EMBO J. 1997; 16:7219–7230. [PubMed: 9405351]

Belfer I, Youngblood V, Darbari DS, Wang Z, Diaw L, Freeman L, Desai K, Dizon M, Allen D, Cunnington C, et al. A GCH1 haplotype confers sex-specific susceptibility to pain crises and altered endothelial function in adults with sickle cell anemia. Am. J. Hematol. 2014; 89:187–193. [PubMed: 24136375]

Bennett GJ, Xie YK. A peripheral mononeuropathy in rat that produces disorders of pain sensation like those seen in man. Pain. 1988; 33:87–107. [PubMed: 2837713]

Bennett DL, Woods CG. Painful and painless channelopathies. Lancet Neurol. 2014; 13:587–599. [PubMed: 24813307]

Bonafé L, Thöny B, Penzien JM, Czarnecki B, Blau N. Mutations in the sepiapterin reductase gene cause a novel tetrahydrobiopterin-dependent monoamine-neurotransmitter deficiency without hyperphenylalaninemia. Am. J. Hum. Genet. 2001; 69:269–277. [PubMed: 11443547]

Chidley C, Haruki H, Pedersen MG, Muller E, Johnsson K. A yeast-based screen reveals that sulfasalazine inhibits tetrahydrobiopterin biosynthesis. Nat. Chem. Biol. 2011; 7:375–383. [PubMed: 21499265]

Chuaiphichai S, McNeill E, Douglas G, Crabtree MJ, Bendall JK, Hale AB, Alp NJ, Channon KM. Cell-autonomous role of endothelial GTP cyclohydrolase 1 and tetrahydrobiopterin in blood pressure regulation. Hypertension. 2014; 64:530–540. [PubMed: 24777984]

Costigan M, Latremoliere A, Woolf CJ. Analgesia by inhibiting tetrahydrobiopterin synthesis. Curr. Opin. Pharmacol. 2012; 12:92–99. [PubMed: 22178186]

Decosterd I, Woolf CJ. Spared nerve injury: an animal model of persistent peripheral neuropathic pain. Pain. 2000; 87:149–158. [PubMed: 10924808]

Dib-Hajj SD, Yang Y, Black JA, Waxman SG. The Na(V)1.7 sodium channel: from molecule to man. Nat. Rev. Neurosci. 2013; 14:49–62. [PubMed: 23232607]

Douglas G, Hale AB, Crabtree MJ, Ryan BJ, Hansler A, Watschinger K, Gross SS, Lygate CA, Alp NJ, Channon KM. A requirement for Gch1 and tetrahydrobiopterin in embryonic development. Dev. Biol. 2015; 399:129–138. [PubMed: 25557619]

Finnerup NB, Otto M, McQuay HJ, Jensen TS, Sindrup SH. Algorithm for neuropathic pain treatment: an evidence based proposal. Pain. 2005; 118:289–305. [PubMed: 16213659]

Finnerup NB, Sindrup SH, Jensen TS. The evidence for pharmacological treatment of neuropathic pain. Pain. 2010; 150:573–581. [PubMed: 20705215]

Friedman PA, Kappelman AH, Kaufman S. Partial purification and characterization of tryptophan hydroxylase from rabbit hindbrain. J. Biol. Chem. 1972; 247:4165–4173. [PubMed: 4402511]

Gorren AC, Mayer B. Tetrahydrobiopterin in nitric oxide synthesis: a novel biological role for pteridines. Curr. Drug Metab. 2002; 3:133–157. [PubMed: 12003347]

Guan Y, Yaster M, Raja SN, Tao YX. Genetic knockout and pharmacologic inhibition of neuronal nitric oxide synthase attenuate nerve injury-induced mechanical hypersensitivity in mice. Mol. Pain. 2007; 3:29. [PubMed: 17922909]

Haruki H, Pedersen MG, Gorska KI, Pojer F, Johnsson K. Tetrahydrobiopterin biosynthesis as an off-target of sulfa drugs. Science. 2013; 340:987–991. [PubMed: 23704574]

Hasegawa H, Abbott S, Han BX, Qi Y, Wang F. Analyzing somatosensory axon projections with the sensory neuron-specific Advillin gene. J. Neurosci. 2007; 27:14404–14414. [PubMed: 18160648]

Heinsbroek SE, Gordon S. The role of macrophages in inflammatory bowel diseases. Expert Rev. Mol. Med. 2009; 11:e14. [PubMed: 19439108]

Hirakawa H, Sawada H, Yamahama Y, Takikawa S, Shintaku H, Hara A, Mase K, Kondo T, Iino T. Expression analysis of the aldoketo reductases involved in the novel biosynthetic pathway of tetrahydrobiopterin in human and mouse tissues. J. Biochem. 2009; 146:51–60. [PubMed: 19273550]

Kayser V, Elfassi IE, Aubel B, Melfort M, Julius D, Gingrich JA, Hamon M, Bourgoin S. Mechanical, thermal and formalin-induced nociception is differentially altered in 5-HT1A−/−, 5-HT1B-−/−, 5-HT2A-−/−, 5-HT3A-−/−, and 5-HTT−/− knock-out male mice. Pain. 2007; 130:235–248. [PubMed: 17250964]

Kim SJ, Lee WI, Lee YS, Kim DH, Chang JW, Kim SW, Lee H. Effective relief of neuropathic pain by adeno-associated virus-mediated expression of a small hairpin RNA against GTP cyclohydrolase 1. Mol. Pain. 2009; 5:67. [PubMed: 19922668]

Kim SK, Kim SH, Nah SS, Lee JH, Hong SJ, Kim HS, Lee HS, Kim HA, Joung CI, Bae J, et al. Association of guanosine triphosphate cyclohydrolase 1 gene polymorphisms with fibromyalgia syndrome in a Korean population. J. Rheumatol. 2013; 40:316–322. [PubMed: 23322459]

Kinne RW, Stuhlmüller B, Burmester GR. Cells of the synovium in rheumatoid arthritis. Macrophages. Arthritis Res. Ther. 2007; 9:224.

Kolinsky MA, Gross SS. The mechanism of potent GTP cyclohydrolase I inhibition by 2,4-diamino-6-hydroxypyrimidine: requirement of the GTP cyclohydrolase I feedback regulatory protein. J. Biol. Chem. 2004; 279:40677–40682. [PubMed: 15292175]

Kuboyama K, Tsuda M, Tsutsui M, Toyohara Y, Tozaki-Saitoh H, Shimokawa H, Yanagihara N, Inoue K. Reduced spinal microglial activation and neuropathic pain after nerve injury in mice lacking all three nitric oxide synthases. Mol. Pain. 2011; 7:50. [PubMed: 21756313]

Latremoliere A, Costigan M. GCH1, BH4 and pain. Curr. Pharm. Biotechnol. 2011; 12:1728–1741. [PubMed: 21466440]

Lee JH, Park CK, Chen G, Han Q, Xie RG, Liu T, Ji RR, Lee SY. A monoclonal antibody that targets a $Na_V1.7$ channel voltage sensor for pain and itch relief. Cell. 2014; 157:1393–1404. [PubMed: 24856969]

Levine RA, Miller LP, Lovenberg W. Tetrahydrobiopterin in striatum: localization in dopamine nerve terminals and role in catecholamine synthesis. Science. 1981; 214:919–921. [PubMed: 6117945]

Li J, Hsu HC, Mountz JD. Managing macrophages in rheumatoid arthritis by reform or removal. Curr. Rheumatol. Rep. 2012; 14:445–454. [PubMed: 22855296]

Marchand F, Perretti M, McMahon SB. Role of the immune system in chronic pain. Nat. Rev. Neurosci. 2005; 6:521–532. [PubMed: 15995723]

McNeill E, Crabtree MJ, Sahgal N, Patel J, Chuaiphichai S, Iqbal AJ, Hale AB, Greaves DR, Channon KM. Regulation of iNOS function and cellular redox state by macrophage Gch1 reveals specific requirements for tetrahydrobiopterin in NRF2 activation. Free Radic. Biol. Med. 2015; 79:206–216. [PubMed: 25451639]

Milstien S, Kaufman S. The biosynthesis of tetrahydrobiopterin in rat brain. Purification and characterization of 6-pyruvoyl tetrahydropterin (2′-oxo)reductase. J. Biol. Chem. 1989; 264:8066–8073. [PubMed: 2656673]

Miyamoto T, Dubin AE, Petrus MJ, Patapoutian A. TRPV1 and TRPA1 mediate peripheral nitric oxide-induced nociception in mice. PLoS ONE. 2009; 4:e7596. [PubMed: 19893614]

Moore PK, Babbedge RC, Wallace P, Gaffen ZA, Hart SL. 7-nitro indazole, an inhibitor of nitric oxide synthase, exhibits anti-nociceptive activity in the mouse without increasing blood pressure. Br. J. Pharmacol. 1993; 108:296–297. [PubMed: 7680591]

Moqrich A, Hwang SW, Earley TJ, Petrus MJ, Murray AN, Spencer KS, Andahazy M, Story GM, Patapoutian A. Impaired thermosensation in mice lacking TRPV3, a heat and camphor sensor in the skin. Science. 2005; 307:1468–1472. [PubMed: 15746429]

Nar H, Huber R, Auerbach G, Fischer M, Hösl C, Ritz H, Bracher A, Meining W, Eberhardt S, Bacher A. Active site topology and reaction mechanism of GTP cyclohydrolase I. Proc. Natl. Acad. Sci. USA. 1995a; 92:12120–12125. [PubMed: 8618856]

Nar H, Huber R, Meining W, Schmid C, Weinkauf S, Bacher A. Atomic structure of GTP cyclohydrolase I. Structure. 1995b; 3:459–466. [PubMed: 7663943]

Nasser A, Bjerrum OJ, Heegaard AM, Møller AT, Larsen M, Dalbøge LS, Dupont E, Jensen TS, Møller LB. Impaired behavioural pain responses in hph-1 mice with inherited deficiency in GTP cyclohydrolase 1 in models of inflammatory pain. Mol. Pain. 2013; 9:5. [PubMed: 23421753]

Nasser A, Ali S, Wilsbech S, Bjerrum OJ, Møller LB. Intraplantar injection of tetrahydrobiopterin induces nociception in mice. Neurosci. Lett. 2015; 584:247–252. [PubMed: 25450138]

Naylor AM, Pojasek KR, Hopkins AL, Blagg J. The tetrahydrobiopterin pathway and pain. Curr. Opin. Investig. Drugs. 2010; 11:19–30.

Nichol CA, Lee CL, Edelstein MP, Chao JY, Duch DS. Biosynthesis of tetrahydrobiopterin by de novo and salvage pathways in adrenal medulla extracts, mammalian cell cultures, and rat brain in vivo. Proc. Natl. Acad. Sci. USA. 1983; 80:1546–1550. [PubMed: 6572916]

O'Dell JR, Mikuls TR, Taylor TH, Ahluwalia V, Brophy M, Warren SR, Lew RA, Cannella AC, Kunkel G, Phibbs CS, et al. CSP 551 RACAT Investigators. Therapies for active rheumatoid arthritis after methotrexate failure. N. Engl. J. Med. 2013; 369:307–318. [PubMed: 23755969]

O'Donovan KJ, Ma K, Guo H, Wang C, Sun F, Han SB, Kim H, Wong JK, Charron J, Zou H, et al. B-RAF kinase drives developmental axon growth and promotes axon regeneration in the injured mature CNS. J. Exp. Med. 2014; 211:801–814. [PubMed: 24733831]

Okamoto K, Imbe H, Morikawa Y, Itoh M, Sekimoto M, Nemoto K, Senba E. 5-HT2A receptor subtype in the peripheral branch of sensory fibers is involved in the potentiation of inflammatory pain in rats. Pain. 2002; 99:133–143. [PubMed: 12237191]

Pickert G, Myrczek T, Rückert S, Weigert A, Häussler A, Ferreirós N, Brüne B, Lötsch J, Tegeder I. Inhibition of GTP cyclohydrolase reduces cancer pain in mice and enhances analgesic effects of morphine. J. Mol. Med. (Berl). 2012; 90:1473–1486. [PubMed: 22706600]

Smith GK, Duch DS, Edelstein MP, Bigham EC. New inhibitors of sepiapterin reductase. Lack of an effect of intracellular tetrahydrobiopterin depletion upon in vitro proliferation of two human cell lines. J. Biol. Chem. 1992; 267:5599–5607. [PubMed: 1544933]

Takazawa C, Fujimoto K, Homma D, Sumi-Ichinose C, Nomura T, Ichinose H, Katoh S. A brain-specific decrease of the tyrosine hydroxylase protein in sepiapterin reductase-null mice—as a

mouse model for Parkinson's disease. Biochem. Biophys. Res. Commun. 2008; 367:787–792. [PubMed: 18201550]

Tatham AL, Crabtree MJ, Warrick N, Cai S, Alp NJ, Channon KM. GTP cyclohydrolase I expression, protein, and activity determine intracellular tetrahydrobiopterin levels, independent of GTP cyclohydrolase feedback regulatory protein expression. J. Biol. Chem. 2009; 284:13660–13668. [PubMed: 19286659]

Tegeder I, Costigan M, Griffin RS, Abele A, Belfer I, Schmidt H, Ehnert C, Nejim J, Marian C, Scholz J, et al. GTP cyclohydrolase and tetrahydrobiopterin regulate pain sensitivity and persistence. Nat. Med. 2006; 12:1269–1277. [PubMed: 17057711]

Thöny B, Blau N. Mutations in the BH4-metabolizing genes GTP cyclohydrolase I, 6-pyruvoyl-tetrahydropterin synthase, sepiapterin reductase, carbinolamine-4a-dehydratase, and dihydropteridine reductase. Hum. Mutat. 2006; 27:870–878. [PubMed: 16917893]

Wagner JA, Williams SA, Webster CJ. Biomarkers and surrogate end points for fit-for-purpose development and regulatory evaluation of new drugs. Clin. Pharmacol. Ther. 2007; 81:104–107. [PubMed: 17186007]

Watschinger K, Keller MA, McNeill E, Alam MT, Lai S, Sailer S, Rauch V, Patel J, Hermetter A, Golderer G, et al. Tetrahydrobiopterin and alkylglycerol monooxygenase substantially alter the murine macrophage lipidome. Proc. Natl. Acad. Sci. USA. 2015; 112:2431–2436. [PubMed: 25675482]

Werner ER, Blau N, Thöny B. Tetrahydrobiopterin: biochemistry and pathophysiology. Biochem. J. 2011; 438:397–414. [PubMed: 21867484]

Woolf CJ. Overcoming obstacles to developing new analgesics. Nat. Med. 2010; 16:1241–1247. [PubMed: 20948534]

Highlights

- Excess BH4 is produced by damaged sensory neurons and macrophages
- Increasing BH4 levels only in DRG neurons produces pain, and blocking it relieves it
- Systemic SPR inhibition reduces chronic pain with no detectable side effects
- Sepiapterin levels correlate with SPR inhibition as a biomarker of target engagement

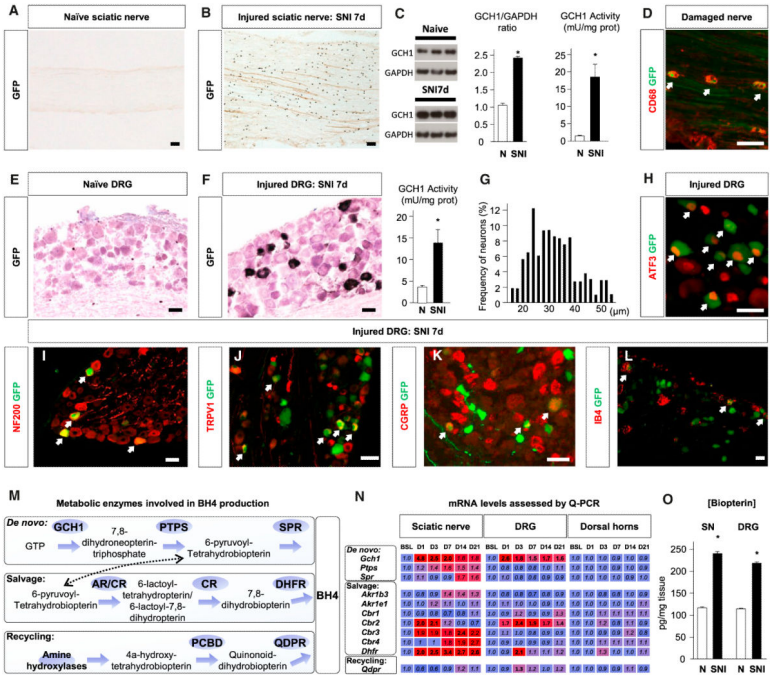

Figure 1. BH4 Synthesis after Nerve Injury

(A and B) eGFP staining in naive sciatic nerve (A) and proximal to nerve lesion 7 days after SNI (B). The scale bars represent 200 μm.

(C) GCH1 protein (n = 9) and GCH1 activity in sciatic nerve (SN) 7 days after SNI (n = 6).

(D) Costaining of GFP with CD68 in SN 7 days after SNI. Arrows indicate double-positive cells. The scale bar represents 50 μm.

(E and F) eGFP staining in naive DRG (E) and 7 days after SNI (F). The scale bars represent 50 μm.

(G) Size distribution of GFP-positive neuron diameters (n = 1,493 neurons) and GCH1 activity (n = 6) in DRG 7 days after SNI. 1 unit (U) = 1 μmol 7,8-dihydroneopterin triphosphate formed per min.

(H–L) Costaining of eGFP with ATF3 (H), NF200 (I), TRPV1 (J), CGRP (K), and IB4 (L) in DRG 7 days after SNI. Arrows indicate double-positive cells. The scale bars represent 50 μm.

(M) Metabolic pathways (de novo, salvage, and recycling) involved in BH4 production.

(N) Quantitative (Q-)PCR time course of enzymes involved in BH4 production in SN, DRG, and dorsal horn after SNI. Numbers indicate fold changes (n = 3 mice per sample; three samples per time point). Bold characters are significant compared to baseline (BSL). Blue indicates no change; red indicates an increase.

(O) Biopterin concentration in SN and DRG 7 days after SNI (n = 40–50).

Mean ± SEM. *$p < 0.05$; two-tailed unpaired Student's t test versus naive condition (C, G, and O); one-way ANOVA followed by Dunnett's post hoc test (N). *Ptps*, pyruvoyl-tetrahydrobiopterin synthase; *Akr1b3/e1*, aldoketo reductase (AR) family 1, member b3/e1; *Crb1–4*, carbonyl reductase 1–4; *Qdpr*, quinoid dihydropteridine reductase; PCBD, pterin-4α-carbinolamine dehydratase. See also Figure S1.

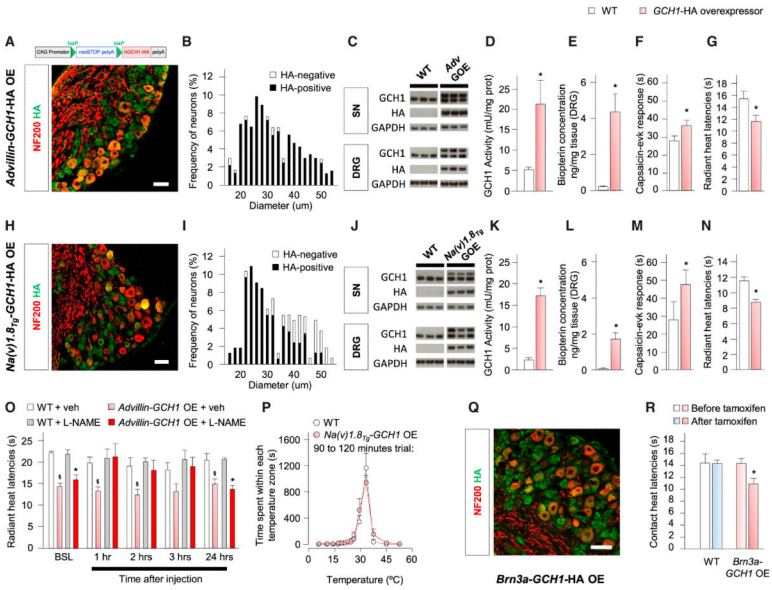

Figure 2. BH4 Overexpression in Sensory Neurons Increases Pain Sensitivity

(A and H) Genetic construct to overexpress *GCH1*-HA (top); costaining of HA (green) with NF200 (red) in DRG of *Advillin-GCH1*-HA OE (A-GOE) (A) and *Na(v)1.8*$_{Tg}$-*GCH1*-HA OE (*N*-GOE) (H) mice.

(B and I) Distribution of HA-positive and -negative neurons in *A*-GOE (B) and *N*-GOE (I) mice (n = 235 and 165 neurons for B and I, respectively).

(C and J) Detection of transgene by western blot using antibodies directed against GCH1 or HA in SN and DRG of *A*-GOE (C) and *N*-GOE (J) mice (n = 3 mice per sample, three samples per condition).

(D and K) GCH1 activity in DRG of *A*-GOE (D) and *N*-GOE (K) mice (n = 3–5; 1 U = 1 μmol 7,8-dihydroneopterin triphosphate formed per min).

(E and L) Biopterin concentration in DRG of *A*-GOE (E) and *N*-GOE (L) mice (n = 3–6).

(F and M) Nocifensive response after intraplantar injection of 1 μg of capsaicin into *A*-GOE (F) and *N*-GOE (M) mice (n = 7–10).

(G and N) Radiant heat withdrawal latencies in *A*-GOE (G) and *N*-GOE (N) mice (n = 8–12).

(O) Radiant heat withdrawal latencies in *A*-GOE mice and littermates after injection of L-NAME (50 mg/kg i.p.; n = 6–9).

(P) Thermal place preference of *N*-GOE mice and littermates on a 4°C–55°C thermal gradient (n = 7–9).

(Q) Costaining of HA (green) with NF200 (red) in DRG of *Brn3a-GCH1*-HA OE mice 1 week after tamoxifen treatment.

(R) Contact heat withdrawal latencies at 52°C in *Brn3a-GCH1*-HA OE mice before and after tamoxifen treatment (n = 6–10).

Mean ± SEM. *p < 0.05; two-tailed unpaired Student's t test compared with littermates (D–G, K–N, and R). *p < 0.05; two-way ANOVA followed by Bonferroni's post hoc test compared with littermates treated with L-NAME (O). §p < 0.05; two-way ANOVA followed by Bonferroni's post hoc test compared with vehicle-treated littermates (O). The scale bars represent 50 μm. See also Figure S2.

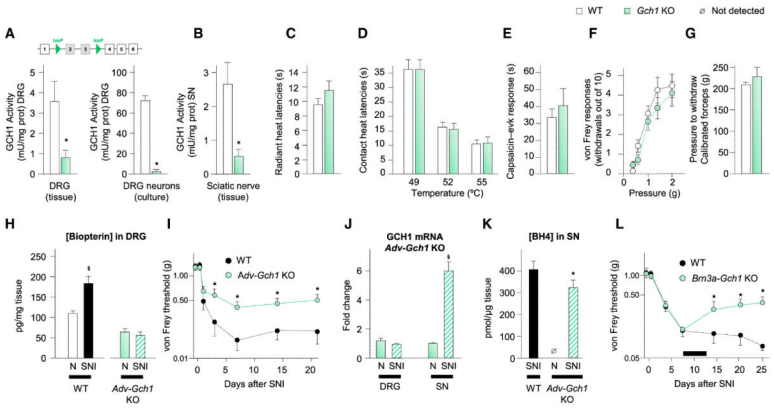

Figure 3. Lack of GCH1 in Sensory Neurons Attenuates Neuropathic Pain-like Symptoms

(A) Top: genetic construct used to excise exons 2 and 3 of *Gch1* upon *Cre*-recombinase exposure. Bottom: GCH1 activity from DRG tissue (left) and primary DRG neuron culture (right) of *Advillin-Gch1* KO mice (n = 3–9).

(B) GCH1 activity from sciatic nerves of KO mice (n = 6–9; 1 U = µmol 7,8-dihydroneopterin triphosphate formed per min).

(C and D) Radiant (C) and contact (D) heat withdrawal latencies in KO mice (n = 8–13).

(E) Nocifensive response after intraplantar injection of 1 µg of capsaicin into KO mice (n = 7–8).

(F) Number of withdrawals out of ten von Frey filament applications to plantar surface of hindpaw in KO mice (n = 11).

(G) Calibrated forceps-elicited withdrawal response in KO mice (n = 12).

(H) Biopterin concentration in DRG of naive KO mice and littermates 7 days after SNI (n = 8–9).

(I) Mechanical hypersensitivity in KO mice and their littermates in the SNI model (n = 12–15).

(J) Q-PCR of Gch1 in sciatic nerve and DRG of KO mice or naive 7 days after SNI (n = 2 mice per sample; three samples per condition).

(K) BH4 levels in sciatic nerve of WT and KO mice after SNI (n = 12–14).

(L) Mechanical hypersensitivity in *Brn3a-Gch1* KO mice and littermates in the SNI model (n = 8–10). The black bar represents the duration of tamoxifen treatment (days 8–13).

Mean ± SEM. *$p < 0.05$; two-tailed unpaired Student's t test compared with littermates (A, B, and K); two-way ANOVA followed by Bonferroni's post hoc test compared with littermates (I and L). §$p < 0.05$; two-tailed unpaired Student's t test compared with uninjured condition of the same genotype (H and J). See also Figure S3.

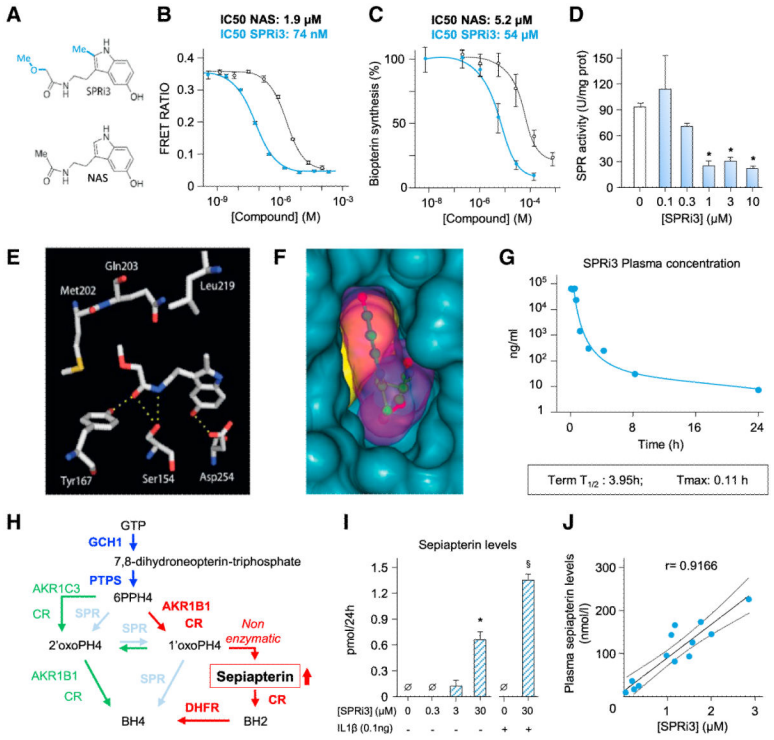

Figure 4. Inhibiting BH4 Production by Targeting SPR

(A) Structure of SPRi3 (top) and NAS (bottom).

(B and C) Concentration-response curves of NAS and SPRi3 binding affinity to SPR tested in vitro by time-resolved fluorescence resonance energy transfer assay (TR-FRET) (B) and reduction of biopterin levels in SK-N-BE(2) neuroblastoma cells (C); 100% synthesis corresponds to biopterin levels after 24 hr incubation with vehicle. Top: calculated IC_{50}.

(D) Sepiapterin reductase activity in DRG neuron cultures after 24 hr incubation with various doses of SPRi3 (n = 3–5 samples per condition; 1 U = µmol sepiapterin consumed per min).

(E) Conformation and interactions of SPRi3 within the substrate-binding site of hSPR (PDB: 4XWY). The four hydrogen bonds between SPRi3 and amino acids of the substrate-binding site are indicated as yellow dotted lines. Hydrophobic interactions are observed between the 2-methyl moiety and Leu219, as well as between the methoxyacetyl group and Met202-Gln203 (image made with MacPyMOL; http://www.pymol.org).

(F) The surfaces of hSPR, SPRi3, and NADPH are indicated as blue, purple, and yellow surfaces, respectively. Shown is a view from the outside looking into the substrate-binding site. Note that the 5-hydroxy group is in close contact with the wall of the binding site.

(G) Plasma levels of SPRi3 in mice after an i.p. injection of 300 mg/kg determined by LC-MS (n = 3 mice per point).

(H) Schematic representation of the enzymatic cascades that form the salvage pathway. Dark blue indicates the de novo pathway that forms 6PPH4 (6-pyruvoyl-tetrahydropterin). SPR (light blue) carries out two reactions to produce BH4. When SPR is absent, 6PPH4 can be metabolized into BH4 through the sequential actions of AKR1C3/CR and AKR1B1/CR (green) or AKR1B1/CR, CR, and DHFR (red). In the latter cascade, the metabolite sepiapterin is formed nonenzymatically from 1′oxoPH4.

(I) Sepiapterin release after inhibition of SPR activity by SPRi3 in DRG neurons (n = 3 samples per condition). In normal conditions or when the de novo pathway is promoted by IL-1β, sepiapterin is not detectable. SPR inhibition leads to increased levels of sepiapterin. (J) Correlation between plasma sepiapterin and SPRi3 levels.

Mean ± SD from triplicate experiments (B and C); mean ± SEM otherwise. *$p < 0.05$; one-way ANOVA followed by Dunnett's post hoc test compared with no SPRi3 condition. §$p < 0.05$; one-tailed Mann-Whitney test compared with no SPRi3 in the presence of IL-1β condition. See also Figure S4.

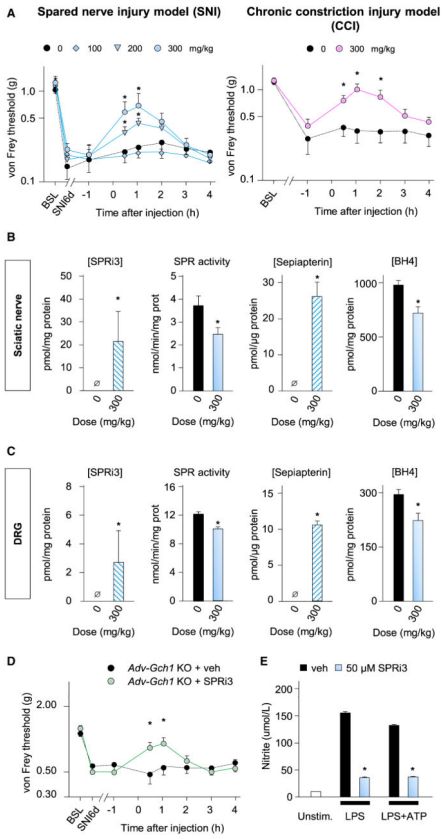

Figure 5. SPR Inhibition Reduces BH4 Levels and Neuropathic Pain Hypersensitivity

(A) Dose-dependent effects of i.p. injections of SPRi3 on mechanical hypersensitivity in mice 7 days post SNI (left; n = 12–14) or 21 days after CCI (right; n = 7–8).

(B and C) One hour after administration of SPRi3, the compound was detected in SN (B) and DRG (C), SPR activity was reduced, sepiapterin levels increased, and BH4 levels were reduced (n = 8–10).

(D) Antiallodynic effects of SPRi3 in *Advillin-Gch1* KO mice 7 days post SNI (n = 8–10).

(E) SPRi3 (50 μM) reduces nitrite production in purified peritoneal macrophages activated by LPS (5 μg/ml) or LPS+ATP (1 mM).

Mean ± SEM. *p < 0.05; two-way ANOVA followed by Bonferroni's post hoc test (A and D). For [SPRi3] and [sepiapterin], one-tailed Mann-Whitney test; for SPR activity and BH4 levels, two-tailed unpaired Student's t test. See also Figure S5.

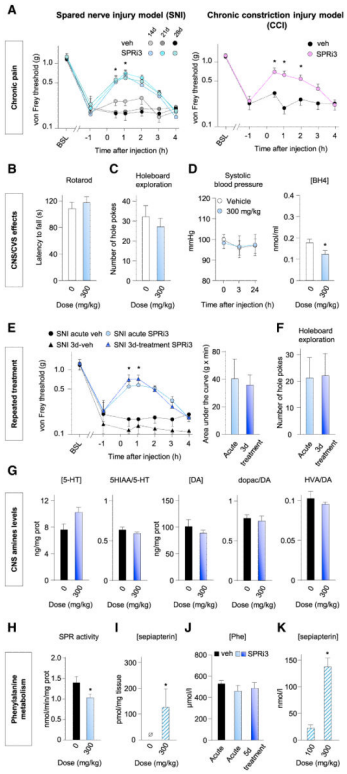

Figure 6. SPR Inhibition Reduces Established Neuropathic Pain Signs without Side Effects

(A) Antiallodynic effects of SPRi3 in SNI mice 14, 21, and 28 days postsurgery (left; n = 7–9) or 6 weeks after CCI (right; n = 7–8).

(B and C) SPRi3 1 hr after injection does not impact rotarod performance (B) or exploration behaviors (C).

(D) SPRi3 does not affect systolic blood pressure 3 and 24 hr postinjection but reduces BH4 plasma levels (n = 8–10).

(E) Mechanical pain thresholds in SNI mice after the first single i.p. administration of SPRi3 (300 mg/kg) and after the last injection of a 3-day regime of bidaily administration at 300 mg/kg (n = 8–9).

(F) Exploration behavior 30 min after the last injection of a 3-day regime of bidaily injections of SPRi3.

(G) Amine levels and the ratio with their metabolites in the striatum 1 hr after the last injection of the 3-day regime (n = 7–9). DA, dopamine; HIAA, 5-hydroxyindoleacetic acid; HVA, homovanillic acid.

(H and I) Sepiapterin reductase activity in liver 1 hr after SPRi3 (H) and sepiapterin levels (I) (n = 4).

(J) Plasma phenylalanine levels 1 hr after vehicle, acute SPRi3 (300 mg/kg i.p.), and last injection of a 5-day regime of bidaily injections of SPRi3.

(K) Plasma sepiapterin level 1 hr after a non-pain-relieving dose of SPRi3 (100 mg/kg) and of a pain-relieving dose (300 mg/kg).

Mean ± SEM. *p < 0.05; two-way ANOVA followed by Bonferroni's post hoc test (A and E); one-tailed Mann-Whitney test (H and I); two-tailed unpaired Student's t test otherwise. See also Figure S6.

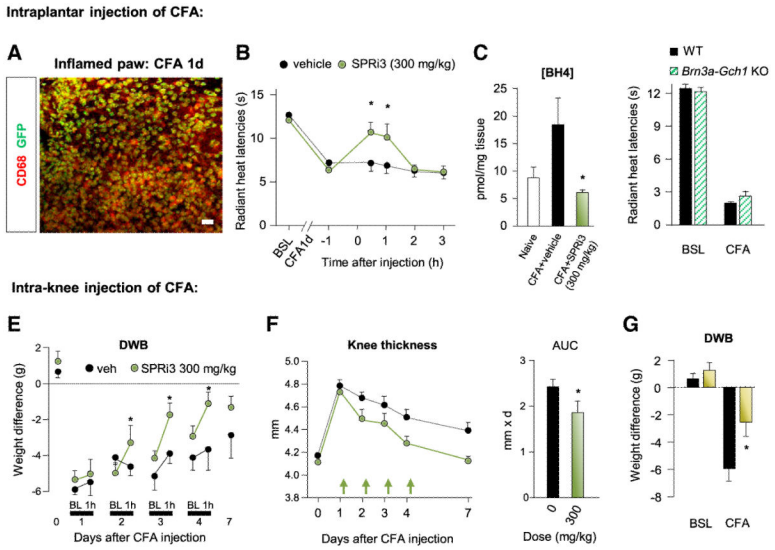

Figure 7. SPR Inhibition Reduces BH4 Levels and Inflammatory Pain Hypersensitivity

(A) Costaining of eGFP with CD68 in paw skin 1 day after intraplantar injection of CFA. The scale bar represents 50 μm.

(B) Effects of SPRi3 on radiant heat latencies 1 day after intraplantar injection of CFA (n = 8).

(C) Effects of SPRi3 on BH4 levels in plantar skin after CFA.

(D) Radiant heat withdrawal latencies in *Brn3a-Gch1* KO mice before and 1 day after intraplantar CFA (n = 5–6).

(E) Effects of SPRi3 on dynamic weight bearing (DWB) 1, 2, 3, and 4 days after CFA injection (n = 5–9). BL, baseline.

(F) Effects of SPRi3 treatment on knee thickness caused by CFA injection into the joint. SPRi3 was administered on day 1, 2, 3, and 4 after CFA injection, and DWB assessment was performed 1 hr later. Each arrow represents an injection. AUC, area under the curve.

(G) Effects of a preemptive treatment with SPRi3 DWB before and 1 day after CFA injection (n = 9).

Mean ± SEM. *p < 0.05; two-way ANOVA followed by Bonferroni's post hoc test (B and E–G); one-way ANOVA followed by Tukey's post hoc test (C). See also Figure S7.